

FIBER QUADRISECANTS IN KNOT ISOTOPIES

T. FIEDLER

*Laboratoire Emile Picard, Université Paul Sabatier,
118 Route Narbonne, 31062 Toulouse, France
fiedler@picard.ups-tlse.fr*

V. KURLIN

*Department of Mathematical Sciences,
Durham University, Durham DH1 3LE, UK
vitaliy.kurlin@durham.ac.uk*

Accepted 28 June 2007

ABSTRACT

Fix a straight line L in Euclidean 3-space and consider the fibration of the complement of L by half-planes. A generic knot K in the complement of L has neither fiber quadriseccants nor fiber extreme secants such that K touches the corresponding half-plane at 2 points. Both types of secants occur in generic isotopies of knots. We give lower bounds for the number of these fiber secants in all isotopies connecting given isotopic knots. The bounds are expressed in terms of invariants calculable in linear time with respect to the number of crossings.

Keywords: Knot; braid; isotopy; fiber quadriseccant; fiber extreme secant; writhe; trace graph; 1-parameter approach; higher order Reidemeister theorem.

Mathematics Subject Classification 2000: 57M25

1. Introduction

In this paper, we give another application of the main result of [3], namely, the *higher order* Reidemeister theorem for one-parameter families of knots. Fix a straight line L in \mathbb{R}^3 , the *axis*. For simplicity assume that L is horizontal. Consider the fibration $\varphi : \mathbb{R}^3 - L \rightarrow S^1_\varphi$ by half-planes attached to the axis L . The fibration φ can be visualized as an open book whose half-planes are fibers of φ . We will study some distances between isotopic knots in the complement $\mathbb{R}^3 - L$.

A knot is the image of a C^∞ -smooth embedding $S^1 \rightarrow \mathbb{R}^3 - L$. An isotopy of knots is a smooth family $\{K_t\}$, $t \in [0, 1]$, of smooth knots. The theory of knots in $\mathbb{R}^3 - L$ covers the classical knot theory in \mathbb{R}^3 and closed braids. An n -braid β is a family of n disjoint strands in a vertical cylinder such that the strands have fixed endpoints on the horizontal bases of the cylinder and they are monotonic in the vertical direction. After identifying the bases of the cylinder in Fig. 1, any braid

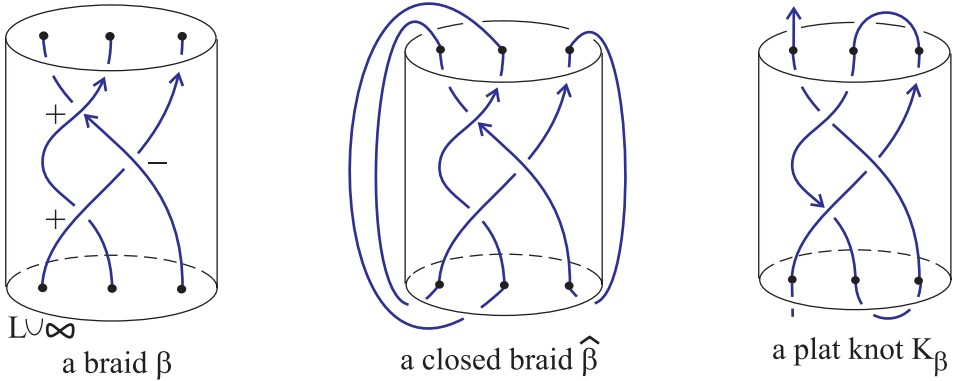


Fig. 1. Examples of a braid, a closed braid, a plat knot.

β becomes a *closed braid* $\hat{\beta}$, a link in a solid torus going around the axis L . The boundary circle of the lower base of the cylinder plays the role of $L \cup \infty$.

A *secant*, a *trisecant* and a *quadriseccant* of $K \subset \mathbb{R}^3 - L$ is a straight line meeting K transversally in 2, 3 and 4 points, respectively. A secant meeting K in points p, q is *extreme* if the secant and the tangents of K at p, q lie in the same plane. Namely, K has tangencies of *order 1* at p, q with a plane passing through the secant, i.e. the plane and K are given by $\{z = 0\}$ and $\{y = 0, z = x^2\}$ in local coordinates near p, q . A generic knot has finitely many extreme secants and quadriseccants. If we are interested only in fiber secants respecting φ , then these geometric features define codimension 1 singularities in the space of all smooth knots $K \subset \mathbb{R}^3 - L$.

Definition 1.1. A *fiber secant*, a *fiber trisecant*, a *fiber quadriseccant* of a knot $K \subset \mathbb{R}^3 - L$ is a straight line meeting K transversally in 2, 3, 4 points, respectively, that lie in a fiber of the fibration $\varphi : \mathbb{R}^3 - L \rightarrow S^1_\varphi$. A fiber secant meeting K in points p, q is called *extreme* if K has tangencies of order 1 at p, q with the fiber.

We use fiber secants to measure a distance between different embeddings of a knot. A similar distance with respect to Reidemeister moves of type III was studied in [1], see Fig. 4. Reidemeister moves can be performed on a knot K in a small neighborhood of a disk. Reidemeister moves III correspond to triple points in the horizontal disk of a projection, i.e. to vertical trisecants meeting K in 3 points.

The authors of [1] found the minimal number of vertical trisecants in isotopies between different representations of a knot. We consider more general features of a knot, namely, quadriseccants in the half-planes of the fibration φ and estimate their minimal number in knot isotopies. Arbitrary quadriseccants provide lower bounds for the ropelength of knots [2]. To define our lower bounds, we associate to each knot $K \subset \mathbb{R}^3 - L$ an oriented graph $TG(K)$, the *trace graph* in a thickened torus.

Choose cylindrical coordinates ρ, φ, λ in \mathbb{R}^3 , where λ is the coordinate on the oriented axis L , ρ and φ are polar coordinates on a plane orthogonal to L . For

an ordered pair of points $(p, q) \in \{\varphi = \text{const}\}$, let $\tau(p, q)$ be the angle between L and the oriented line $S(p, q)$ passing first through p and after through q . Denote by $\rho(p, q)$ the distance between $S(p, q)$ and the origin $0 \in L$. Introduce the oriented thickened torus $\mathbb{T} = S^1_\tau \times S^1_\varphi \times \mathbb{R}^+_rho$ parametrized by $\tau, \varphi \in [0, 2\pi)$ and $\rho \in \mathbb{R}^+$.

Definition 1.2. Take a knot $K \subset \mathbb{R}^3 - L$ in general position such that K intersects each fiber of φ in finitely many points. Map an ordered pair $(p, q) \in K \cap \{\varphi = \text{const}\}$ to $(\tau(p, q), \varphi, \rho(p, q)) \in \mathbb{T}$. So, each oriented fiber secant of K maps to a point in the thickened torus \mathbb{T} . The image of this map is the *trace graph* $\text{TG}(K) \subset \mathbb{T}$.

Figure 2 shows the trace graph $\text{TG}(K)$ of a long trefoil K going once around a distant horizontal circle $L \cup \infty$. The fibers there are horizontal planes. The trace graph $\text{TG}(K)$ can be visualized as a trace of fiber secants evolving along K . The knots in Fig. 2 are obtained from K by the rotation around a vertical line. A crossing in the projection of a rotated knot corresponds to a fiber secant of K , i.e. to a point of $\text{TG}(K)$. The embedding $\text{TG}(K) \subset \mathbb{T}$ is symmetric under the shift $\tau \mapsto \tau + \pi$. This shift reverses the orientation of each fiber secant.

For a generic knot K of Definition 2.1, $\text{TG}(K)$ can have only *hanging* vertices \bullet and *triple* vertices \times associated to fiber tangents and fiber trisecants

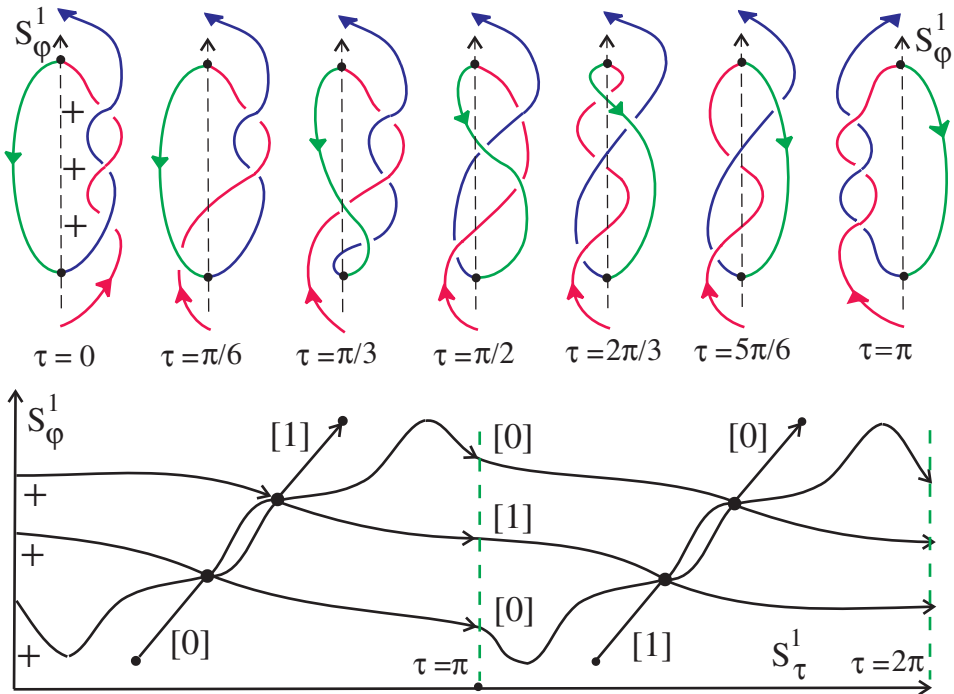


Fig. 2. The trace graph $\text{TG}(K)$ of a long trefoil K .

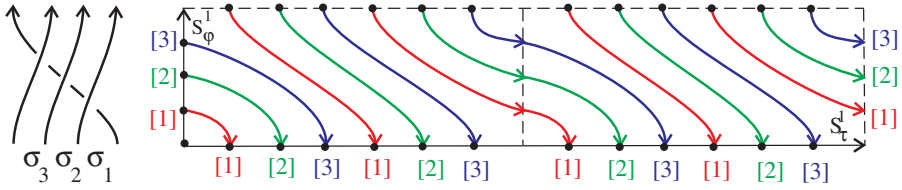


Fig. 3. The trace graph of $\widehat{\sigma_3\sigma_2\sigma_1}$ splits into 3 trace circles.

of K , respectively. A double crossing of $\text{TG}(K)$ under $\text{pr}_{\tau\varphi} : \text{TG}(K) \rightarrow S_\tau^1 \times S_\varphi^1$ corresponds to a pair of parallel secants meeting K in points that lie in a fiber $\{\varphi = \text{const}\}$.

Let m be the linking number of a knot K with the axis L . It turns out that the trace graph $\text{TG}(K)$ splits into a union of oriented *traces* (arcs or circles) marked by canonically defined homological markings in $\mathbb{Z}_{|m|}$, where $\mathbb{Z}_0 = \mathbb{Z}$ and $\mathbb{Z}_1 = \{0\}$, see Definition 2.2. For example, the closure of $\sigma_3\sigma_2\sigma_1 \in B_4$ has the trace graph in Fig. 3, which is a disjoint union of 3 trace circles marked by $[1], [2], [3] \in \mathbb{Z}_4$.

Introduce the *sign* of a crossing in the projection $\text{pr}_{\tau\varphi}(\text{TG}(K))$ as usual, see Fig. 1. We shall define 3 functions on $\text{TG}(K)$, which will be invariant under regular isotopy of $\text{TG}(K)$, not allowing Reidemeister moves of type I, see Lemma 3.1.

Definition 1.3. Take a knot $K \subset \mathbb{R}^3 - L$ such that $\text{lk}(K, L) = m \neq \pm 1$ and the projection $\text{pr}_{\tau\varphi}(\text{TG}(K))$ has finitely many crossings. For distinct $[a], [b] \in \mathbb{Z}_{|m|} - \{0\}$, the *unordered writhe* $W_{a,b}^u(K)$ is the sum of signs over all crossings of the trace marked by $[a]$ with the trace $[b]$. The *ordered writhe* $W_{a,b}^o(K)$ is the sum of signs over all crossings, where the trace $[a]$ crosses over the trace $[b]$. The *coordinated writhe* $W_{a,a}^c(K)$ is the sum of signs over all self-crossings of the trace $[a]$.

We do not consider knots $K \subset \mathbb{R}^3 - L$ with $\text{lk}(K, L) = \pm 1$, because in this case $\text{TG}(K)$ splits into trace arcs marked by $[0]$ and $[1]$ only, see Definition 2.2. The trace graph $\text{TG}(K)$ can be constructed from a plane projection of K , see Lemma 2.4. The writhes of Definition 1.3 depend on a geometric embedding $K \subset \mathbb{R}^3 - L$, but can be computed in linear time with respect to the number of crossings of K and change under knot isotopies in a controllable way, see Lemma 3.2.

Theorem 1.4. For isotopic generic knots $K_0, K_1 \subset \mathbb{R}^3 - L$, denote by $\text{fqs}(K_0, K_1)$ and $\text{fes}(K_0, K_1)$ the least number of fiber quadrisecants and fiber extreme secants, respectively, occurring during all isotopies $\{K_t\}$, $t \in [0, 1]$.

For isotopic knots K_0, K_1 , we have $\text{fqs}(K_0, K_1) \geq \frac{1}{12} \sum_{0 \neq a \neq b \neq 0} |W_{a,b}^u(K_0) - W_{a,b}^u(K_1)|$ and $\text{fqs}(K_0, K_1) + \frac{1}{6} \text{fes}(K_0, K_1) \geq \frac{1}{12} \sum_{a \neq 0} |W_{a,a}^c(K_0) - W_{a,a}^c(K_1)|$. Given isotopic closed braids $\hat{\beta}_0, \hat{\beta}_1$, we get $\text{fqs}(\hat{\beta}_0, \hat{\beta}_1) \geq \frac{1}{12} \sum_{0 \neq a \neq b \neq 0} |W_{a,b}^o(\hat{\beta}_0) - W_{a,b}^o(\hat{\beta}_1)|$.

The third lower bound is not less than the first one, but works for closed braids only. The second bound gives another estimate for the number of fiber quadrisecants for closed braids since fiber extreme secants do not occur in braid isotopies. In Example 3.3, we show that the second lower bound can be arbitrarily large.

The lower bounds for the least number of Reidemeister moves III are computed with exponential complexity in [1], while the writhes of Definition 1.3 can be computed in linear time with respect to the number of crossings, see Lemma 2.4. Other applications of the 1-parameter approach to knot theory [3] are in [4, 5].

2. The Trace Graph of a Knot

We shall define generic knots $K \subset \mathbb{R}^3 - L$ and geometric features of knots, considered as codimension 1 singularities in the space of all knots in $\mathbb{R}^3 - L$. Each singularity is illustrated by a small portion of the projection of K along the corresponding secant. For example, a tangent of K maps to a cusp Υ in the plane projection along the tangent, while a quadrisecant projects to a quadruple point \ast .

Definition 2.1. A knot $K \subset \mathbb{R}^3 - L$ is *generic* if K has **no** following features:

- \ast : a fiber quadrisecant intersecting K transversally in 4 points;
- \times : a fiber trisecant meeting K in 3 points such that the trisecant lies in the plane spanned by the tangents of K at 2 of these points;
- Υ : a fiber secant meeting K in 2 points and having a tangency of order 1 with K at one of these points;
- \mathcal{J} : a fiber secant meeting K in points p, q such that K has a tangency of order 2 at p with the plane spanned by the secant and the tangent of K at q , i.e. the plane and K are given by $\{z = 0\}$ and $\{y = 0, z = x^3\}$ in local coordinates near p ;
- \curvearrowright : a fiber tangent having a tangency of order 2 with K at p , i.e. the tangent and K are given by $\{y = z = 0\}$ and $\{y = 0, x^2 = z^5\}$ in local coordinates near p ;
- \times, \ast : a fiber trisecant meeting K in 3 points such that K has a tangency of order 1 with the fiber at one of these points;
- \curvearrowleft : a fiber tangent meeting K in a point, where K has a tangency of order 2 with the fiber, i.e. the fiber and K are given locally by $\{z = 0\}$ and $\{y = 0, z = x^3\}$;
- $\curvearrowright, \curvearrowleft$: a fiber secant meeting K in 2 points, where K has tangencies of order 1 with the fiber.

The singularities of Definition 2.1 can be visualized by rotating a knot around a vertical line. The last singularity represents two local extrema $\wedge \wedge$ with the same vertical coordinate: they collide under the projection after a suitable rotation.

A *trace* in the trace graph $TG(K)$ of a knot K is either a subarc ending at hanging vertices or a subcircle of $TG(K)$. A trace passes through triple vertices without changing its direction. The trace graph in Fig. 2 consists of 2 trace arcs.

By Definition 1.2, any point in $TG(K)$ corresponds to a fiber secant of K and also to an intersection in the projection of K along the secant. Hanging vertices and

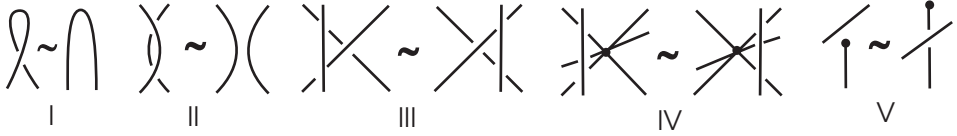


Fig. 4. Reidemeister moves for trace graphs.

triple vertices of $TG(K)$ correspond to cusps Υ and triple intersections \bowtie , respectively. Mark also *tangent* vertices ζ of degree 2 in $TG(K)$ whose corresponding secants project to tangent points of order 1, see 2 tangent vertices in Fig. 6(iv).

All points of $TG(K)$ apart from the vertices of $TG(K)$ correspond to double crossings with well-defined signs. Associate to such a general point, the *sign* of the corresponding crossing in the projection. Two close points of $TG(K)$ on different sides of a tangent vertex correspond to a couple of crossings with opposite signs like in Reidemeister move II, see Fig. 4. While we travel along a trace of $TG(K)$, the sign does not change at triple vertices, but is reversed at tangent vertices.

To be completely honest we should also consider *critical* vertices \curvearrowright of degree 2 in $TG(K)$ corresponding to a critical crossing \blacktriangleright in a projection of K . Then K has a fiber secant and another fiber tangent in the same fiber. These critical vertices are local extrema of $\text{pr}_\varphi : TG(K) \rightarrow S^1_\varphi$ and denoted by small empty circles in Fig. 6. The critical vertices of $TG(K)$ will not play any role further.

Let us look at the function τ on fiber secants passing through 2 points p, q on K . Namely, $\tau(p, q)$ is the angle between L and the fiber secant through p, q . The function $\tau(p, q)$ has a local extremum if and only if the corresponding secant of K projects to a tangent point, i.e. τ changes its monotonic type at tangent vertices of $TG(K)$. So, passing through a tangent point of $TG(K)$ reverses the sign of crossing in the projection of K and simultaneously the monotonic type of τ .

Definition 2.2. Take a generic knot $K \subset \mathbb{R}^3 - L$ with $\text{lk}(K, L) = m$. Split $TG(K)$ by tangent vertices into arcs with associated signs coming from plane projections. Orient each arc so that if the angle τ increases (respectively, decreases) along the arc then the associated sign of the arc is $+1$ (respectively, -1), see Fig. 2.

Any point of $TG(K)$ apart from the vertices of $TG(K)$ is associated to a crossing (p, q) in the projection of K along the secant through $p, q \in K$. Smoothing crossing (p, q) produces a diagram of a 2-component link. The linking number of the circle $L \cup \infty$ with the component in which the undercrossing goes to the overcrossing in the original projection of K is called the *homological marking* $[a] \in \mathbb{Z}_{|m|}$ of (p, q) and of the point of $TG(K)$, see Fig. 3.

The trace graph in Fig. 2 splits into 2 trace arcs marked by $[0]$ and $[1]$. Under the shift $\tau \mapsto \tau + \pi$, the homological marking $[a]$ becomes $[|m| - a] \in \mathbb{Z}_{|m|}$, see Fig. 3. Recall that a hanging vertex of $TG(K)$ corresponds to a fiber tangent of K , i.e. to an ordinary cusp in the plane projection along this tangent.

Lemma 2.3. *The trace graph $TG(K)$ of a generic knot K splits into traces with well-defined homological markings. The orientation of edges, introduced in Definition 2.2, provides orientations of all traces of $TG(K)$.*

Proof. Consider the sign of a crossing, monotonic type of the function τ and homological marking as functions of a point in the trace graph $TG(K)$. All these functions remain constant while the projection of K along the corresponding secant keeps its combinatorial type. By the classical Reidemeister theorem, a knot projection can change under Reidemeister moves of types I–III, see Fig. 4.

Under Reidemeister move I, a fiber secant of K appears or disappears, i.e. the corresponding point in the trace graph comes to a hanging vertex. Under Reidemeister move II, two crossings with opposite signs and the same marking appear or disappear. At this moment the function τ reverses its monotonic type. So the orientations of adjacent arcs of $TG(K)$ agree at tangent vertices. Under Reidemeister move III, nothing changes, i.e. all arcs of a trace have the same marking. \square

The right picture in Fig. 1 shows a *plat* diagram of a knot K_β associated to a braid β . Any knot can be isotoped to a curve having a plat diagram.

Lemma 2.4. *Let K_β be a knot with a plat diagram associated to a $(2n + 1)$ -braid β of braid length l . The trace graph $TG(K_\beta)$ can be constructed combinatorially from the diagram of K_β . The writhe of Definition 1.3 can be computed with complexity Cln^2 , where the constant C does not depend on l and n .*

Proof. We describe the trace graphs of elementary braids containing one crossing only. Figure 5 shows the explicit example of the crossing σ_1 of first two strands in the 4-braid. Firstly, we draw all strands in a vertical cylinder. Secondly, we approximate with the first derivative the strands forming a crossing by smooth arcs.

The monotonic strands in the left pictures of Fig. 5 are denoted by 1, 2, 3, 4. The trace graphs in the right pictures have arcs labeled by ordered pairs (ij) , $i, j \in \{1, 2, 3, 4\}$. The arc (ij) represents crossings, where the i th strand crosses over the j th one. For instance, at the moment $\tau = 0$ the braid σ_1 has exactly one crossing (12) , which becomes crossing (21) after rotating the braid through $\tau = \pi/4$. Two triple vertices on the upper right picture correspond to two fiber (horizontal) trisecants in the upper left picture. Similarly, we construct the trace graph of a local extremum. The only hanging vertex corresponds to a horizontal tangent.

In general, we split K_β by fibers of $\varphi : \mathbb{R}^3 - L \rightarrow S_\varphi^1$ into several sectors each of that contains exactly one crossing or one extremum. To each sector we associate the corresponding elementary block and glue them together. The resulting trace graph contains $2l(2n - 1)$ triple vertices and $2n$ hanging vertices. Any two arcs in an elementary block have at most one crossing, not more than n^2 crossings in total. So each writhe of Definition 1.3 can be computed with complexity Cln^2 . \square

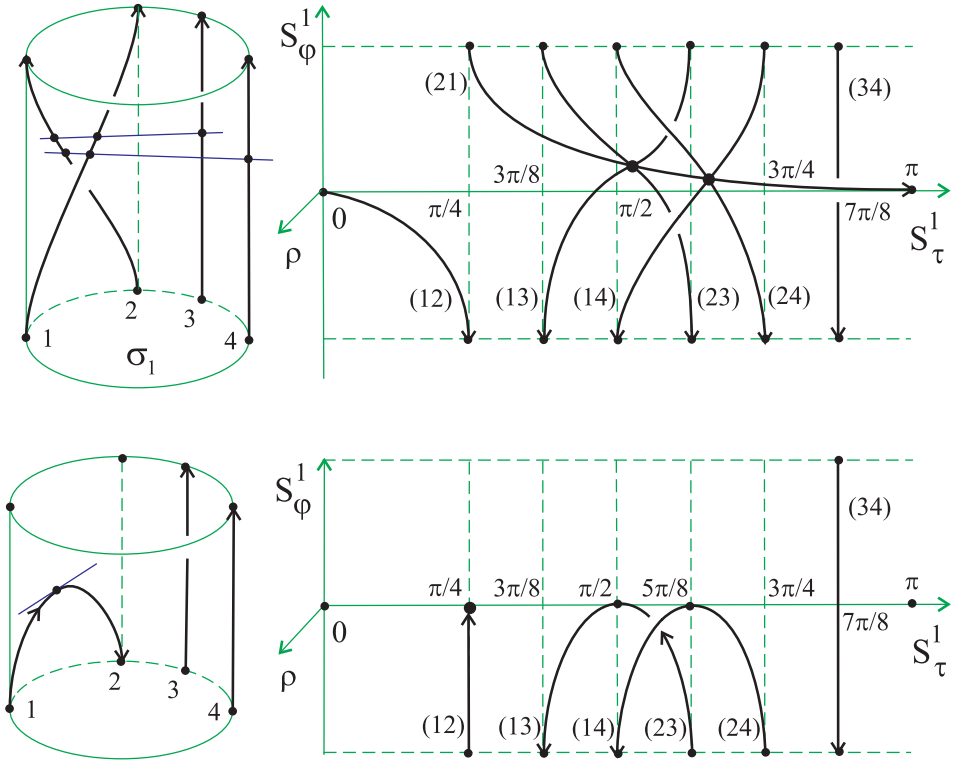


Fig. 5. Half trace graphs of $\sigma_1 \in B_4$ and a local maximum.

Definition 2.5. Denote by Ω the discriminant of knots K failing to be generic due to one of the singularities of Definition 2.1. An isotopy of knots $\{K_t\}$, $t \in [0, 1]$, is *generic* if the path $\{K_t\}$ intersects Ω transversally. A *regular* isotopy of trace graphs is generated by isotopy in $S_\tau^1 \times S_\varphi^1$ and Reidemeister moves II–V.

Any orientations and symmetric images of the moves in Fig. 4 are allowed. Proposition 2.6 is a particular case of the more general higher order Reidemeister theorem [3, Sec. 1.3]. A knot can be reconstructed from its trace graph equipped with labels, ordered pairs of integers, see details in [3, Sec. 6.1].

Proposition 2.6. *If knots $K_0, K_1 \subset \mathbb{R}^3 - L$ are isotopic, then $TG(K_0), TG(K_1)$ are related by regular isotopy and a finite sequence of the moves in Fig. 6.*

Proof. The singularities of Definition 2.4 are all essential codimension 1 singularities associated to fiber secants and fiber tangents of knots, see [3, Sec. 3]. There are also codimension 1 singularities formed by pairs of fiber secants and fiber tangents

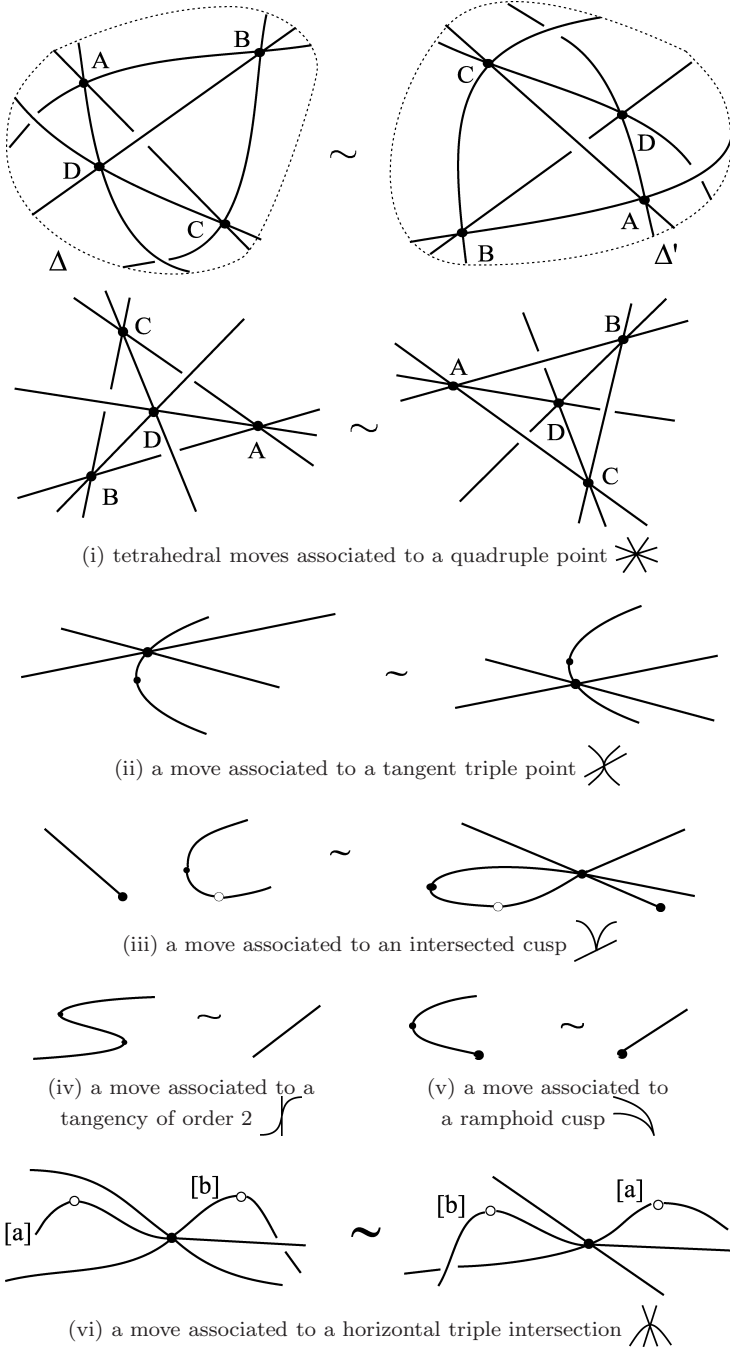


Fig. 6. Moves on trace graphs.

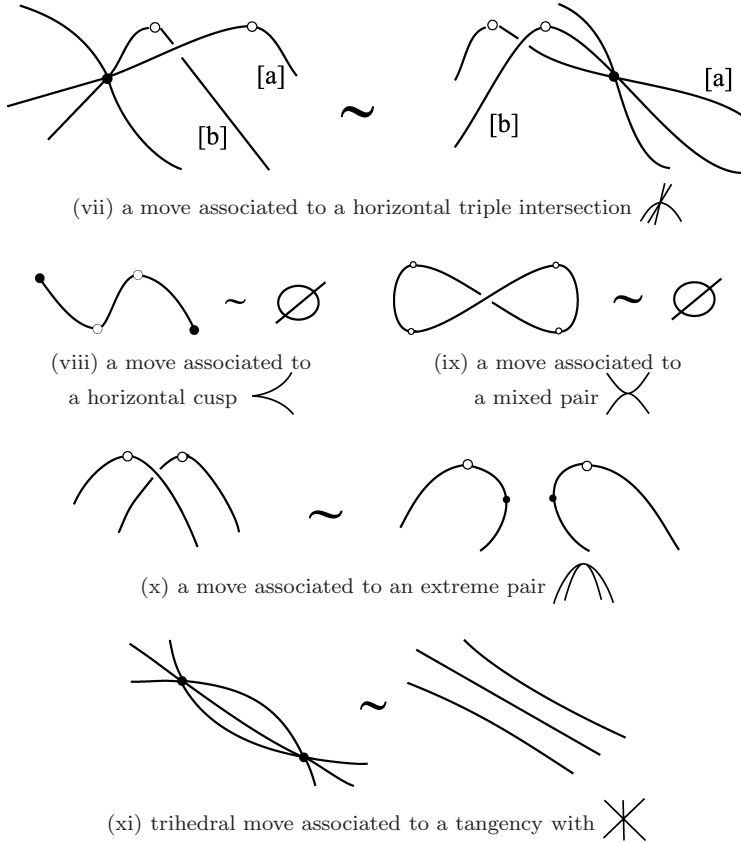


Fig. 6. (Continued)

in the same fiber, but they give rise to trivial moves on trace graphs. For example, the singularity $\mathbb{X} \curvearrowright$, where a fiber secant and a fiber tangent are in the same fiber, leads to the move throwing an arc over a critical vertex.

Any isotopy of knots can be approximated by a generic isotopy of Definition 2.5. Each move of Fig. 6 corresponds to one of the singularities. For instance, when a path in the space of knots passes through a knot with a fiber quadrisequant, the tetrahedral move 6i changes the trace graph by collapsing and blowing up the 1-skeleton of a tetrahedron. A formal correspondence between the singularities and moves was shown in [3, Lemma 5.5].

The moves of Fig. 6 keep the orientation and homological markings of traces. If three traces marked by $[a], [b], [c]$ meet in a triple vertex then $b = a + c \pmod{|m|}$, where $[b]$ is the marking of the middle trace, see [5, Lemma 3.3]. The trace graph always remains symmetric under $\tau \mapsto \tau + \pi$. Hence, each move of Fig. 6 describes how to replace a small disk Δ and the symmetric image of Δ under $\tau \mapsto \tau + \pi$ by another small disk Δ' and the symmetric image of Δ' , respectively. \square

3. Proofs of Main Results

Lemma 3.1. *The writhes of Definition 1.3 are invariant under regular isotopy of trace graphs in the sense of Definition 2.5.*

Proof. The Reidemeister moves of types II–IV in Fig. 4 do not change the sum of signs in the writhes. The Reidemeister move of type V either adds or deletes a crossing of $TG(K)$, but a trace arc coming to a hanging vertex always has homology marking $[0]$ modulo $|\text{lk}(K, L)|$ and is excluded in Definition 1.3. \square

Lemma 3.2. *The moves in Fig. 6 keep the writhes of Definition 1.3 except*

- *the move 6(i) changes $W_{a,b}^u$ ($a \neq b$) by ± 2 for at most 6 unordered pairs $\{a, b\}$;*
- *the move 6(i) changes $W_{a,b}^o$ ($a \neq b$) by ± 1 for at most 12 ordered pairs (a, b) ;*
- *the move 6(i) changes $W_{a,a}^c$ either (1) by ± 6 for at most 2 values of a , or (2) by ± 4 for at most 2 values of a and by ± 2 for at most 2 values of a , or (3) by ± 2 for at most 6 values of a ;*
- *the moves 6(vi), 6(vii) change $W_{a,b}^o$ ($a \neq b$) by ± 1 for at most 4 ordered pairs (a, b) ;*
- *the moves 6(ix) and 6(x) change $W_{a,a}^c$ by ± 1 for at most two values of a .*

Proof. No crossings appear or disappear in the moves 6(ii)–6(v), 6(viii) and 6(xi). The move 6(i) reverses exactly 3 couples of symmetric crossings. For instance, the arc DB crosses over AC in the left picture of Fig. 6(i), but DB crosses under AC in the right picture. Hence, for at most 6 unordered pairs $\{a, b\}$ with $a \neq b$, the unordered writhe $W_{a,b}^u$ changes by ± 2 . Similarly, for at most 12 ordered pairs (a, b) , the ordered writhe $W_{a,b}^o$ changes by ± 1 since exactly one crossing of a trace $[a]$ over a trace $[b]$ either appears or disappears under the move 6(i).

If all the 3 crossings in the disk Δ in Fig. 6(i) are formed by traces with the same homological marking $[a]$, then the coordinated writhes $W_{a,a}^c$ and $W_{|m|-a, |m|-a}^c$ change by ± 6 as required in (1). If two of the above crossings are formed by a trace $[a]$ and the remaining one by a different trace $[b]$, then we arrive at (2). The case (3) arises when each of the 3 crossings in Δ is formed by a different trace.

In the moves 6(vi) and 6(vii), the overcrossing arc becomes undercrossing and vice versa, but the sign of the crossing is invariant, i.e. $W_{a,b}^u$ does not change. Each of the moves 6(vi) and 6(vii) deletes exactly one crossing, where a trace $[a]$ crosses over a trace $[b]$, and adds another crossing, where the trace $[a]$ crosses under the trace $[b]$. Under the symmetry $\tau \mapsto \tau + \pi$, we get similar conclusions for the traces marked by $[|m| - a]$ and $[|m| - b]$. So the ordered writhe $W_{a,b}^o$ changes by ± 1 for the 4 ordered pairs (a, b) , (b, a) and $(|m| - a, |m| - b)$, $(|m| - b, |m| - a)$.

The move 6(ix) adds or deletes a crossing of a trace circle $[a]$ with itself. Hence, only the writhes $W_{a,a}^c$ and $W_{|m|-a, |m|-a}^c$ change by ± 1 . The move 6(x) adds or

deletes a crossing between arcs that belong to traces with the same homological marking $[a]$. Indeed, a pair of crossings corresponding to these arcs looks like a horizontal version \curvearrowright of Reidemeister move II, see Fig. 4. By Definition 2.2, the markings of these crossings are equal. So the conclusion is the same as for the move 6(ix). \square

Proof of Theorem 1.4. To prove the first lower bound, it suffices to show that the right-hand side increases by 1 only if a generic isotopy $\{K_t\}$ passes through a knot with a fiber quadriseccant. By Lemma 3.2, the unordered writhe changes under the move 6(i) associated to a fiber quadriseccant, see the correspondence between singularities and moves in [3, Lemma 5.5]. Six unordered pairs $\{a, b\}$ provide the maximal increase 1 as required. Lemma 3.2 also proves the third lower bound since only the moves 6(i), 6(ii), 6(iv), 6(xi) are relevant for braids.

For the second lower bound, we are interested in crossings whose arcs have the same marking. By Lemma 3.2, the coordinated writhe changes only under the move 6(i) and two moves 6(ix), 6(x) associated to a fiber extreme secant in knot isotopies. Under the move 6(i), the right-hand side increases at most by 1 while under the moves 6(ix) and 6(x) the maximal increase is $1/6$ after multiplying by $1/12$. \square

Example 3.3. Consider the isotopic closures of the braids $\beta_0 = \sigma_3\sigma_2\sigma_1$ and $\beta_1 = (\sigma_1\sigma_3\sigma_2)^2\sigma_3^{-1}\sigma_2^{-1}\sigma_3^{-1}$. The trace graphs of $\hat{\beta}_0$ and $\hat{\beta}_1$ are in Fig. 3 and Fig. 7,

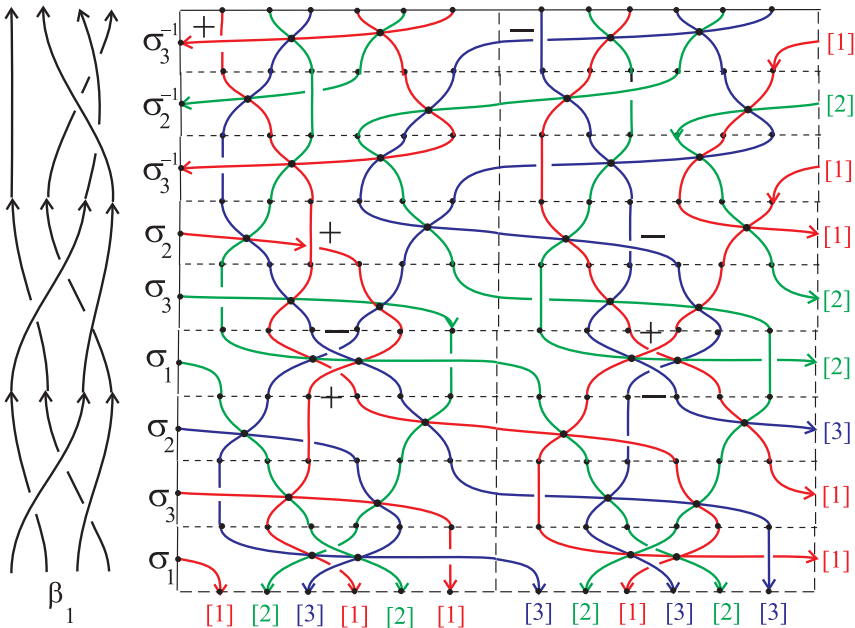


Fig. 7. The trace graph of the closure of $\beta_1 = (\sigma_1\sigma_3\sigma_2)^2\sigma_3^{-1}\sigma_2^{-1}\sigma_3^{-1}$.

respectively. They were constructed by attaching elementary blocks described in the proof of Lemma 2.4. So we assume that the closed braids are given by embeddings into a neighborhood of the torus $S^1_\tau \times S^1_\varphi$ located vertically in $\mathbb{R}^3 - L$.

Both graphs split into 3 closed traces (circles with self-intersections) marked by [1], [2], [3]. The trace graph in Fig. 3 has no crossings, i.e. the writhes of Definition 1.3 vanish. For the trace graph of $\hat{\beta}_1$, the non-zero writhes are $W_{1,1}^c = 4$, $W_{3,3}^c = -4$. The 4 signs + and 4 signs - are shown in Fig. 7. The second lower bound of Theorem 1.4 implies that any isotopy connecting the closed braids $\hat{\beta}_0, \hat{\beta}_1$ involves at least one fiber quadriseccant. The conclusion is the same for the closures of $\beta_0\gamma, \beta_1\gamma$, where γ is any pure 4-braid, i.e. the permutation generated by γ is trivial.

Consider the 4-braid $\beta = (\sigma_1\sigma_3\sigma_2)^2(\sigma_1^{-1}\sigma_3^{-1}\sigma_2^{-1})^2$ in Fig. 8 and the sequence of the braids $\beta_n = \beta^{n-1}\beta_1$, $n \geq 1$, whose closures are isotopic to $\hat{\beta}_0$, see Fig. 3. Figure 8 contains the part of $TG(\hat{\beta}_n)$ corresponding to a single factor β in β_n . So $TG(\hat{\beta}_n)$ is obtained from $TG(\hat{\beta}_1)$ by inserting $n-1$ copies of Fig. 8 at the bottom of Fig. 7. The part in Fig. 8 has the writhes $W_{1,1}^c = 3$ and $W_{3,3}^c = -3$. Hence, $TG(\hat{\beta}_n)$

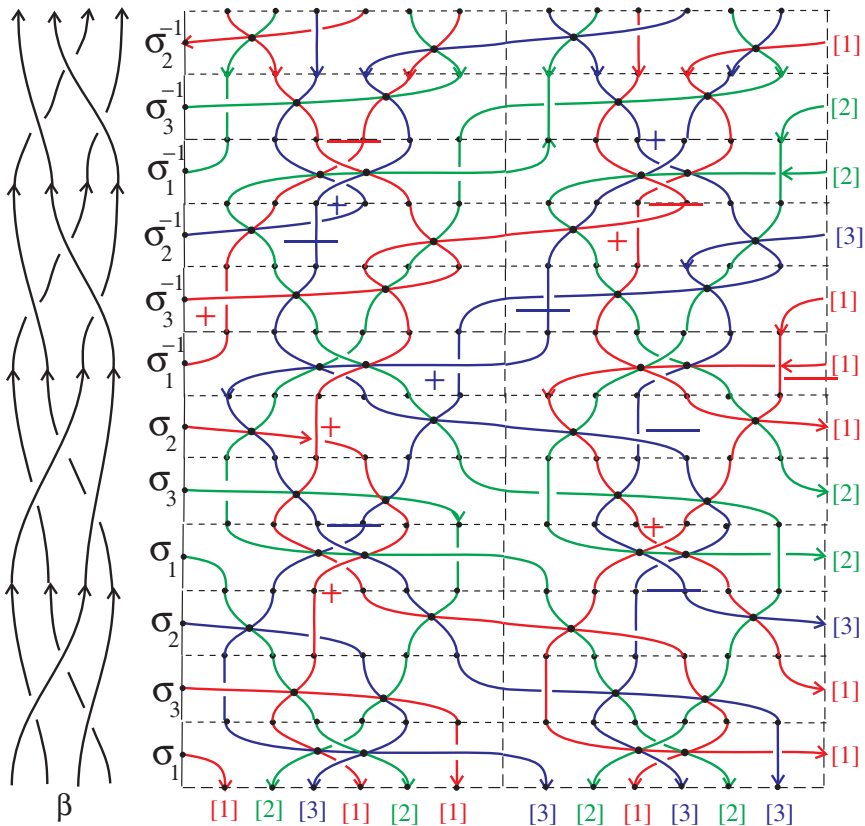


Fig. 8. The part of the trace graph for the factor $\beta = (\sigma_1\sigma_3\sigma_2)^2(\sigma_1^{-1}\sigma_3^{-1}\sigma_2^{-1})^2$.

has $W_{1,1}^c = 3n + 1$ and $W_{3,3}^c = -3n - 1$. By Theorem 1.4, any isotopy connecting the closures of β_0 and β_n involves at least $\frac{3n+1}{12}$ fiber quadriseccants. So the second lower bound of Theorem 1.4 can be arbitrarily large.

Acknowledgments

The authors thank Hugh Morton and the anonymous referee for useful comments. The second author was supported by Marie Curie Fellowship 007477.

References

- [1] J. S. Carter, M. Elhamdadi, M. Saito and S. Satoh, A lower bound for the number of Reidemeister moves of type III, *Topol. Appl.* **153** (2006) 2788–2794.
- [2] E. Denne, Y. Diao and J. M. Sullivan, Quadriseccants give new bounds for ropelength, *Geom. Topol.* **10** (2006) 1–26.
- [3] T. Fiedler and V. Kurlin, A one-parameter approach to knot theory, preprint, math.GT/0606381.
- [4] T. Fiedler, Isotopy invariants for closed braids and almost closed braids via loops in stratified spaces, preprint, math.GT/0606443.
- [5] T. Fiedler and V. Kurlin, Recognizing trace graphs of closed braids, preprint, arXiv: 0808.2713.